Journal of proteome research

Article

pubs.acs.org/jpr

# Comparative Proteomic Analysis of Human Liver Tissue and Isolated Hepatocytes with a Focus on Proteins Determining Drug Exposure

Anna Vildhede,[†] Jacek R. Wiśniewski,[§] Agneta Norén,[‡] Maria Karlgren,[†] and Per Artursson*[,†,∥]

[†]Department of Pharmacy and [‡]Department of Surgery, Uppsala University, 751 05 Uppsala, Sweden

[§]Biochemical Proteomics Group, Department of Proteomics and Signal Transduction, Max Planck Institute of Biochemistry, 82152 Martinsried, Germany

[∥]Uppsala University Drug Optimization and Pharmaceutical Profiling Platform (UDOPP), Chemical Biology Consortium, Science for Life Laboratory, 750 03 Uppsala, Sweden

*S* *Supporting Information*

**ABSTRACT:** Freshly isolated human hepatocytes are considered the gold standard for in vitro studies of liver functions, including drug transport, metabolism, and toxicity. For accurate predictions of the in vivo outcome, the isolated hepatocytes should reflect the phenotype of their in vivo counterpart, i.e., hepatocytes in human liver tissue. Here, we quantified and compared the membrane proteomes of freshly isolated hepatocytes and human liver tissue using a label-free shotgun proteomics approach. A total of 5144 unique proteins were identified, spanning over 6 orders of magnitude in abundance. There was a good global correlation in protein abundance. However, the expression of many plasma membrane proteins was lower in the isolated hepatocytes than in the liver tissue. This included transport proteins that determine hepatocyte exposure to many drugs and endogenous compounds. Pathway analysis of the differentially expressed proteins confirmed that hepatocytes are exposed to oxidative stress during isolation and suggested that plasma membrane proteins were degraded via the protein ubiquitination pathway. Finally, using pitavastatin as an example, we show how protein quantifications can improve in vitro predictions of in vivo liver clearance. We tentatively conclude that our data set will be a useful resource for improved hepatocyte predictions of the in vivo outcome.

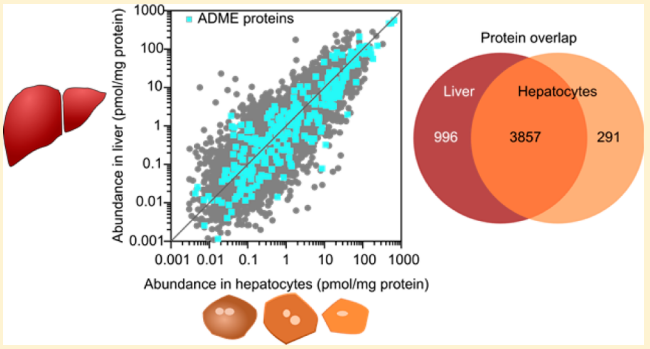


**KEYWORDS:** *quantitative proteomics, total protein approach, oxidative stress, human hepatocytes, membrane proteome, ADME proteins, CYP enzymes, UGT enzymes, drug transporters, in vitro−in vivo extrapolation*

## INTRODUCTION

The liver is the major detoxifying organ. Because it clears most drugs and other xenobiotics, it determines the efficacy and toxicity associated with drug exposure. During the last decades, drug-induced liver injury has been the most frequent cause of safety-related drug marketing withdrawals in the US.[1] Hepatotoxicity discovered in late stages of drug development has also restricted the use, or even prevented the approval, of many drugs.[2] Large efforts are therefore made to develop in vitro methods that predict drug fate and toxicity in vivo. In such efforts, freshly isolated hepatocytes are considered the gold standard against which emerging models, such as hepatocyte-like stem cells and more complex co-cultures with nonparenchymal cells, are compared.[3−5]

Individual susceptibility for adverse drug reactions is to a large extent explained by differences in drug exposure, which, in turn, most often depends on the extent of liver clearance (CL). Factors affecting liver CL include the activities of drug-metabolizing enzymes and transport proteins involved in the drug disposition. These and other so-called ADME proteins have thus been a focus of interest in pharmacokinetic research as a major factor for explaining adverse drug reactions and variability in drug response.[6]

Knowledge of both protein abundance and function is key for understanding drug metabolism and transporter-mediated distribution. Nevertheless, there are few quantitative global expression analyses of proteins that determine hepatic exposure. This is partly related to technical issues. Most ADME proteins are integral membrane proteins, which complicates their analysis. Furthermore, important ADME proteins, such as transport proteins in the plasma membrane, are often expressed in low amounts, making their detection and quantification difficult. Recent advances in instrumentation and sample preparation have improved the sensitivity and throughput of liquid chromatography−tandem mass spectrometry (LC−MS/MS) analysis to a level that allows almost complete proteome coverage.[7] As a result, accurate determinations of protein levels from label-free LC−MS/MS

**Received:** April 20, 2015
**Published:** July 13, 2015

  

DOI: 10.1021/acs.jproteome.5b00334
*J. Proteome Res.* 2015, 14, 3305−3314

analysis are now feasible using the total protein approach.[8,9] Advantages of the label-free approach include the large number of proteins that are quantified simultaneously and the dynamic range of detection.

For accurate predictions of drug fate and toxicity, the in vitro model must accurately reflect the phenotype of hepatocytes in vivo. Whereas primary rat hepatocytes differ from rat liver tissue on the basis of the mRNA expression profile,[10] freshly isolated human hepatocytes are reported to have a similar profile to human liver tissue.[11] Given that only 40% of the variation in protein abundance is explained by mRNA levels,[12] an analysis of the similarity in protein expression profiles for isolated hepatocytes and liver tissue is motivated. Although Wimmer et al. presented a comparative proteome study including hepatocytes and liver tissue at a qualitative level,[13] the hepatocyte and liver tissue proteomes have, to our knowledge, not previously been compared quantitatively.

Herein, we performed in-depth, quantitative LC−MS/MS analysis of the membrane proteome of human liver tissue and freshly isolated hepatocytes, with a focus on proteins that determine hepatic drug exposure. Freshly isolated hepatocytes were selected for the analysis to distinguish isolation-related changes from culture-dependent proteome changes.[14,15] Our analysis revealed that proteins in the endoplasmic reticulum membrane, including many hepatocyte-specific drug metabolizing cytochrome P450 (CYP) enzymes, were retained during isolation and sample preparation. In contrast, the levels of hepatocyte-specific drug transporters and many other proteins present in the plasma membrane were lower in the primary cells compared to those in liver tissue. A lower fraction of mitochondrial membrane proteins in the isolated hepatocytes was also observed. Pathway analysis of those proteins for which expression levels differed significantly support previous observations that the hepatocytes are exposed to oxidative stress during isolation.[16,17] Moreover, altered protein expression was associated with the protein ubiquitination pathway, which may explain the reduced levels of plasma membrane proteins. Using the protein abundance data, we show that primary hepatocytes are likely to underpredict the in vivo CL of pitavastatin and other drugs that are dependent on transporters for their hepatic elimination. We propose a simple approach for extrapolating in vitro data to predict in vivo outcome.

## MATERIALS AND METHODS

### Human Liver Tissue and Primary Cells

Samples of normal human liver tissue were obtained from 20 donors undergoing surgical resections carried out at the Department of Surgery, Uppsala University Hospital in Uppsala, Sweden. Donors gave informed consent. Ethical approval was granted by the Uppsala Regional Ethics Committee (ethical approval no. 2009/028). A total of 12 of the tissue samples were snap-frozen immediately after excision and stored at −80 °C. These samples were used for global proteomic analysis of liver tissue as described below. The remaining tissue samples were used for the isolation of hepatocytes and subsequent global proteomic analysis. The hepatocytes were isolated according to the two-step collagenase isolation procedure described elsewhere.[18] The isolations lasted for approximately 3 h (from the start of the isolation to the freezing of the cell pellets) and resulted in an average yield of 8 million hepatocytes/g liver with a viability of 82%. Isolated hepatocytes were pelleted by centrifugation at 75*g* for 5 min. The resulting cell pellet was washed once with Dulbecco's phosphate buffered saline and stored at −80 °C until further analysis.

### Proteomic Analysis

**Liver Membrane Fractions.** Crude membrane fractions were isolated from frozen liver tissue by consecutive extractions of liver homogenate with 2 M NaCl, 0.01 M $NaCO_3$, and 4 M urea as described elsewhere.[19] The membrane fractions were lysed in 0.1 M Tris−HCl at pH 7.6, 4% (w/v) SDS, and 0.1 M DTT. Aliquots containing 50 $\mu$g of total protein were processed in 30 kDa ultrafiltration units (MRCF0R030, Millipore)[20] according to the filter-aided sample preparation procedure.[21] The ratio of total protein to trypsin was 100:1. Aliquots of 6 $\mu$g of the trypsin-digested peptides were brought to pH 11 with 1× Britton−Robinson Universal Buffer (BRUB, 0.1 M $CH_3COOH$, 0.1 M $H_3PO_4$, and 0.1 M $H_3BO_3$, adjusted with NaOH to pH 11). The samples were subsequently loaded into pipet-tip SAX microcolumns as described[22] and then washed with 200 $\mu$L of 0.2× BRUB. The peptides were eluted with 100 $\mu$L of 0.1% $CF_3COOH$ into StageTip C18 columns.[23] The SAX fractionation step was necessary for the removal of unknown polar substances affecting the liquid chromatography. Peptide concentrations were determined spectrofluorometrically using tryptophan as a standard.[24]

**Hepatocyte Membrane Fractions.** Hepatocytes were homogenized in 10 mM Tris−-HCl at pH 7.8, 0.25 M sucrose, 5 mM $MgCl_2$, and protease inhibitors (Complete Tablets, Roche, Basel, Switzerland), and clarified by centrifugation (2000*g*, 10 min). The supernatant was ultracentrifuged at 200000*g* at 4 °C for 30 min. The resulting crude membrane fractions were lysed and processed as described above except that the ion exchange step was omitted.

**LC−MS/MS Analysis.** The peptides were separated on a reverse phase column (20 cm × 75 $\mu$m inner diameter) packed with 1.8 $\mu$m C18 particles (Dr. Maisch GmbH, Ammerbuch-Entringen, Germany) using a 4 h acetonitrile gradient in 0.1% formic acid at a flow rate of 250 nL/min. The liquid chromatography was coupled to a LTQ Orbitrap Velos instrument (Thermo Fisher Scientific, Germany) via a Proxeon nanoelectrospray ionization source. The mass spectrometer was operated in data-dependent mode with full scan acquisition in the Orbitrap at a resolution of 30 000 at 400 $m/z$. For the data-dependent scans, the 10 most intense ions were selected with assigned charge state ≥+2. The maximum ion injection times for the full scan and the MS/MS scans were 20 and 60 ms, respectively. The ion target value for both scan modes were set to $10^6$. The dynamic exclusion was 95 s and 10 ppm.

**Data Analysis.** The spectra were searched using the MaxQuant software version 1.2.6.20 and the "matching between runs" option.[25] Proteins were identified by searching MS and MS/MS data of peptides against the UniProtKB/Swiss-Prot database (May 2013) containing 50 807 sequences. As part of the searches, FDR was determined by analyzing the decoy database. Carbamidomethylation of cysteines was set as a fixed modification. *N*-terminal acetylation and oxidation of methionines were set as variable modifications. Up to two missed cleavages were allowed. The allowed mass deviation was initially up to 6 ppm for the precursor ion and 0.5 Da for the fragment masses. The mass accuracy of the precursor ions was improved by time-dependent recalibration algorithms of MaxQuant. The "matching between runs" option enabled us to match identifications across samples within a time window of 2 min of the aligned retention times. The maximum false peptide discovery rate was set at 0.01.



DOI: 10.1021/acs.jproteome.5b00334
*J. Proteome Res.* 2015, 14, 3305−3314

**Protein Quantification.** The raw protein intensities of the MaxQuant output were used for the calculation of protein concentrations according to the total protein approach[26] using the relationship:

$$\text{protein concentration(i)} = \frac{\text{MS signal(i)}}{\text{total MS signal} \times M_w\text{(i)}} \left[\frac{\text{mol}}{\text{g total protein}}\right] \quad \text{(eq 1)}$$

where "MS signal(i)" refers to the total MS1 signal intensity of protein i, and "total MS signal" refers to the summed MS1 signals of all proteins.

### Collection of CYP, UGT, and Transporter Abundance Data

Recently, two meta-analyses have summarized CYP and uridine 5′-diphospho-glucuronosyltransferase (UGT) enzyme abundance levels in Caucasian adults.[27,28] Here, we refined the analysis to include only the samples with measurable levels of expression. In addition, the highest abundances measured for the UGT enzymes were corrected by including the range of the study by Sato et al.[29]

PubMed was searched with appropriate keywords (e.g., liver and hepatic transporter quantification, abundance, and expression, etc.) to find relevant studies reporting transport protein abundance in human liver tissue. The data compiled from the literature search are summarized in Table S1 in the Supporting Information. A weighed mean of liver tissue abundance was calculated as described in the enzyme meta-analyses.[27,28]

### In Vitro–in Vivo Scaling of Pitavastatin Uptake Clearance Using Protein Abundance Data

Pitavastatin uptake CL in isolated hepatocytes and human liver tissue was predicted as described previously.[30,31] Briefly, transport kinetics was studied in human embryonic kidney (HEK) 293 cells stably overexpressing each of the uptake transporters involved in the hepatic disposition of pitavastatin. The measured maximal transport rate ($V_{max}$) in the transfected HEK293 cells was then used to estimate the maximal transport activity (MTA) or $V_{max}$ in human hepatocytes by incorporating a scaling factor accounting for the difference in transporter abundance (as shown in eq 2). The MTA in liver tissue was subsequently derived by scaling the hepatocyte prediction with the ratio of transporter abundance in liver tissue to that in isolated hepatocytes as determined by label-free quantification. Intrinsic transporter-mediated uptake clearance ($CL_{int,uptake}$) was calculated according to eq 3.

$$\text{MTA} = \frac{\text{Protein expression}_{\text{hepatocytes}}}{\text{Protein expression}_{\text{HEK293cells}}} \times V_{max(\text{HEK293cells})} \quad \text{(eq 2)}$$

$$CL_{int,uptake} = \sum_{\text{transporters}} \frac{\text{MTA}}{K_m + [S]_u} \quad \text{(eq 3)}$$

where MTA represents the estimated $V_{max}$ in the various systems (isolated hepatocytes and liver tissue), $K_m$ is the substrate concentration at which the uptake rate is half of $V_{max}$, and $[S]_u$ is the maximal unbound plasma concentration of pitavastatin. A value of 88 mg protein/g liver[31] was used to scale the data to whole liver.

### Prediction of Pitavastatin Uptake Clearance from External Transporter Abundance Data

As an external validation of our prediction method, the reported expression levels of NTCP,[32] OATP1B1, OATP1B3, and OATP2B1[33] in a pooled batch of cryopreserved hepatocytes were used to predict pitavastatin uptake CL from the in vitro HEK293 kinetic data (see above). The prediction was compared to the reported uptake CL.[33]

### Statistical Analysis and Bioinformatics

Donor data were described by proportion, median, and interquartile range. Differences between the donor groups were judged by Fisher exact or Mann–Whitney tests as appropriate.

**Gene Ontology Enrichment Analysis.** Proteins varying the most and the least (on the basis of the coefficient of variation) in abundance in either of the two groups (i.e., the top and bottom 10%) were subjected to gene ontology (GO) category enrichment analysis using Perseus version 1.5.0.8 (http://www.perseus-framework.org/). A Benjamini–Hochberg false discovery ratio of 0.01 was used as a measure of statistical significance.

**Pathway Analysis of Differentially Expressed Proteins.** Proteins with a significant change in abundance in the two sample groups were identified by a two-sample $t$ test as implemented in Perseus version 1.5.0.8. A permutation-based false discovery ratio of 0.05 (1000 permutations) was used to define statistical significance. Bioinformatic analysis of the differently expressed proteins was performed with Ingenuity Pathway Analysis (IPA) software version 21901358 (Ingenuity Systems, Redwood City, CA, USA, http://www.ingenuity.com); the analysis was restricted to experimental observations for human liver tissue or hepatocytes. Canonical pathways most significantly associated with the altered proteins were identified from the IPA library of canonical pathways. The statistical data were generated by the software.

## RESULTS

### Donor Characteristics

Normal (nontumorous) liver tissue was obtained from donors undergoing partial hepatectomy. The samples were either snap-frozen within 10 min of excision or used for hepatocyte isolations. The demographics of the donors are summarized in Table 1. The donors had a median age of 62 years (interquartile range of 58–68), and there was an equal distribution between males and females. There were no differences between the donor groups with regards to age ($p = 0.53$), gender ($p = 0.65$), or cytostatic treatment ($p = 0.37$). Importantly, there were no differences in protein expression levels for patients that had obtained cytostatic treatment before surgery and those that underwent liver resections without prior cytostatic treatment. This is in agreement with a separate study in which cytostatic treatment given 6 weeks prior to surgery was reported to have

**Table 1. Donor Demographics Divided by Sample Group**

| characteristic | liver, $n = 12$ | hepatocytes, $n = 8$ | all, $n = 20$ |
|---|---|---|---|
| age, median (IQR)[a] | 65 (58–69) | 60 (54–67) | 62 (58–68) |
| gender | | | |
| male | 7 (58%) | 3 (37.5%) | 10 (50%) |
| female | 5 (42%) | 5 (62.5%) | 10 (50%) |
| diagnosis[b] | | | |
| CRC | 10 (83.3%) | 8 (100%) | 18 (90%) |
| HCC | 1 (8.3%) | 0 | 1 (5%) |
| GynCa | 1 (8.3%) | 0 | 1 (5%) |
| cytostatic treatment | 6 (50%) | 6 (75%) | 12 (60%) |

[a]IQR, interquartile range. [b]CRC, colorectal cancer; HCC, hepatocellular cancer; GynCa, gynecological cancer.



DOI: 10.1021/acs.jproteome.5b00334
J. Proteome Res. 2015, 14, 3305–3314

minimal effects on the proteome of nontumorous liver tissue,[34] nor did gender influence the protein levels.

## Membrane Proteome of Human Liver Tissue and Isolated Human Hepatocytes

To investigate the molecular events occurring during hepatocyte isolation, we performed quantitative proteomic analysis by in-depth label-free mass spectrometry on both sample types (see Figure 1A). More than 5000 proteins were identified, of which 75% (3857 of 5144) were found in both sample types (Figure 1B). The 2000 most abundant proteins constituted >99% of the membrane proteins by mass (Figure S1, Supporting Information), indicating a sufficient depth of analysis for accurate protein abundance calculations.[8] The measured protein abundances spanned 6 orders of magnitude, but the levels for 98% of the proteins were within a 10 000-fold expression range (Figure 1C). Overall, a good global correlation in membrane protein abundance was observed for the two sample types (Figure 1D).

**Absence of Nonparenchymal Cells in the Hepatocyte Preparations.** Using cell-specific markers, we investigated the purity of the isolated hepatocytes (Figure 1E). All markers of nonparenchymal liver cells showed less abundance in hepatocyte samples than in liver tissue. For example, the three markers of liver sinusoidal endothelial cells decreased in abundance to a level of 2.7−6.3% of that in human liver tissue. At the same time, hepatocyte markers remained or increased in abundance, indicating a proper purification of hepatocytes.

**Hyper- and Hypovariable Membrane Proteins.** Variation in protein abundance for the two groups was quantified by calculating the coefficient of variation. Membrane proteins varying the most in abundance were found to be enriched in GO categories associated with immune response-related biological processes, whereas the least variable were related to essential processes, such as the establishment of protein localization. A subset of the proteins displaying the lowest variability in abundance is shown in Figure 1F.

**Protein Abundance in the Various Cell Membrane Types.** Membrane proteins were classified into their respective subcellular localization by GO annotations. No significant differences in the fraction of membrane proteins associated with the endoplasmic reticulum and peroxisomes were observed for the two groups. Plasma membrane proteins and mitochondrial proteins, however, constituted less of the total membrane fraction in hepatocytes than in liver tissue (Figure 2A). The plasma membrane fraction was more reduced than the mitochondrial one. For example, the well-known plasma membrane marker CD81 showed a 4-fold lower abundance in hepatocytes (Figure 2B).

**Associations between Altered Proteins and Canonical Pathways.** To obtain information about the underlying biology behind the reduced plasma membrane and mitochondrial membrane fractions, we investigated proteins with a significant change in abundance by pathway analysis. The top canonical pathway associated with up-regulated proteins in hepatocyte samples was eukaryotic initiation factor 2 (eIF2) signaling ($p = 2.6{\cdot}10^{-22}$), which was predicted to be activated ($z$-score of 4.9). A variety of stimuli, including oxidative stress, modulates eIF2 activity, which in turn regulates mRNA translation. NRF2-mediated oxidative stress response was also predicted to be activated in the isolated hepatocytes ($z$-score of 3.9), as shown in Figure S2 in the Supporting Information. These findings support previous observations of oxidative stress responses during isolation[17] and suggest that the hepatocytes responded by activating the transcription of detoxifying proteins. Up-regulated proteins were also associated with the protein ubiquitination pathway ($p = 1.9{\cdot}10^{-12}$), which is involved in protein degradation (Figure 2C), and the mTOR signaling pathway ($p = 2.1{\cdot}10^{-9}$), which is involved in cell survival and proliferation. The top canonical pathways associated with the down-regulated proteins in the hepatocyte samples were oxidative phosphorylation ($p = 6.8{\cdot}10^{-33}$) and mitochondrial dysfunction ($p = 8.5{\cdot}10^{-33}$). In addition, integrin signaling was predicted to be inactivated ($z$-score of −4.2), which is in agreement with the inevitable disruption of cell−matrix contact during isolation.

## Proteins Determining Hepatocyte Exposure to Drugs

From a list of close to 700 genes coding for proteins with relevance for ADME,[35] about half were detected in the human liver and hepatocyte samples (Figure 1B). The ADME proteins represented 7.0 ± 0.2% of the total number of identified proteins but as much as 24.0 ± 4.2% of the membrane protein mass, highlighting the importance of hepatocytes in drug detoxification.

The ADME protein abundance in the isolated hepatocytes correlated positively with that in the liver tissue (Figure 1D). In line with this, we detected comparable amounts of endoplasmic reticulum-localized drug metabolizing CYP and UGT enzymes in the two groups (Figure 3A,B), many of which are hepatocyte-specific. Interindividual variability in the expression of drug-metabolizing CYP enzymes is known to affect exposure to many drugs. The interindividual differences in our material ranged from 3.3- (for CYP4F2) to 2230-fold for the highly polymorphic enzyme CYP2D6.

In contrast to the metabolizing enzymes, drug transporters in the plasma membrane were generally less abundant in the isolated hepatocytes than in the liver tissue (Figure 3C). The difference was particularly large (2- to 5-fold lower in the hepatocytes) for the hepatocyte-specific transporters organic anion transporting polypeptide (OATP) 1B1 (*SLCO1B1*), OATP1B3 (*SLCO1B3*), sodium−taurocholate cotransporting polypeptide (NTCP, *SLC10A1*), and bile salt export pump (BSEP, *ABCB11*). Clearly, the loss of plasma membrane proteins was not obscured by the presence of other cell types in the liver tissue samples.

Of the three groups of ADME proteins presented above, CYP enzymes showed the highest abundances, followed by UGT enzymes. Transport proteins were in general one to 2 orders of magnitude less abundant than the phase I (CYP) and phase II (UGT) metabolizing enzymes.

## Comparison of Measured Abundance Levels with Literature Data

Measured protein levels of enzymes and transporters were compared with literature data. Because of the similarity in CYP and UGT expression in liver tissue and hepatocytes, the mean abundance from all the samples was used. Expression levels of drug-metabolizing CYP and UGT enzymes matched the data from two recent meta-analyses that used various other quantitative or semiquantitative techniques, including targeted LC−MS/MS, Western blot, and ELISA (Figure 3D,E). The median absolute fold difference of our measured mean abundances compared to the weighed means from the meta-analyses was 2.2. Importantly, there was no trend of either over- or underestimating protein abundance, as indicated by an average fold difference of 1.2. Only UGT2B15 had an average abundance that was lower than the reported meta-analysis range. UGT2B15 levels were, however, likely underestimated herein because the protein was identified by a single unique peptide.



DOI: 10.1021/acs.jproteome.5b00334
J. Proteome Res. 2015, 14, 3305−3314

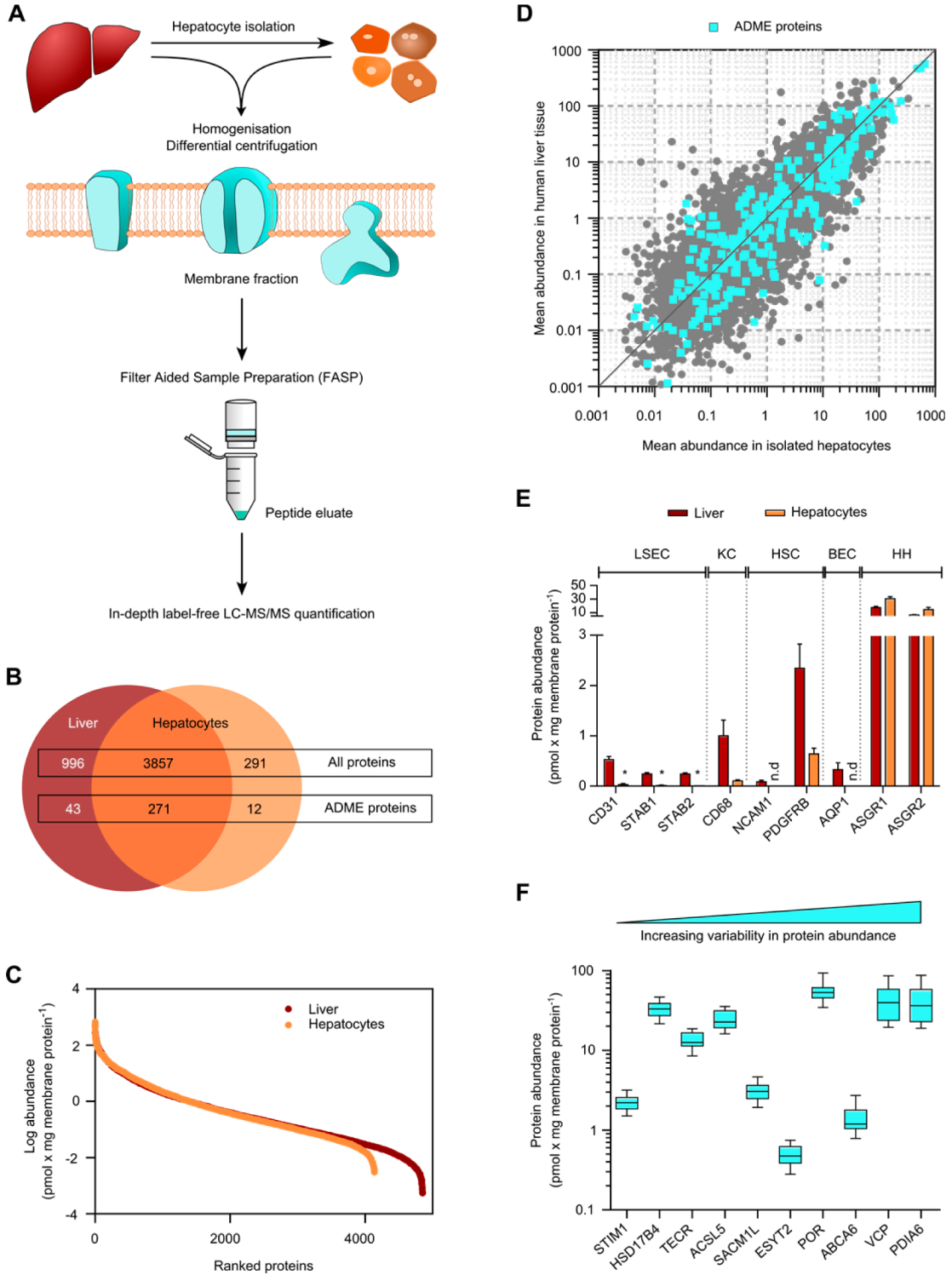


**Figure 1.** In-depth proteomic analysis of human liver tissue and isolated human hepatocytes. (A) Proteomic workflow applied to the samples. (B) Overlap of proteins identified in the human liver and hepatocyte membrane fractions. (C) Ranked protein abundances from the highest to the lowest in liver and hepatocyte samples. (D) Correlation of protein abundances for the two groups. The global correlation in protein expression was $r^2$ = 0.63, and even higher ($r^2$ = 0.92) for the ADME proteins. (E) Protein abundance of cell specific markers. Markers for the nonparenchymal cells of the liver (LSEC, liver sinusoidal endothelial cells; KC, Kuppfer cells; HSC, human stellate cells; BEC, biliary endothelial cells) were less abundant in isolated hepatocytes than liver. Human hepatocyte (HH) markers, however, were enriched in the hepatocyte samples. n.d, not detected; *, $p < 0.01$. (F) Boxplot of a subset of proteins displaying the lowest interindividual variability in abundance. The whiskers represent the range in expression.

Although there are fewer studies quantifying hepatic drug transporters, our liver tissue expression levels were mostly in the same range (Figure 3F), especially for proteins that have been quantified in more than a single study. For the nine transporters with reported abundances in more than 70 liver samples, the median absolute fold difference was only 1.5. These results support the accuracy of the total protein approach-based, label- and standard-free protein quantifications.



DOI: 10.1021/acs.jproteome.5b00334
J. Proteome Res. 2015, 14, 3305−3314

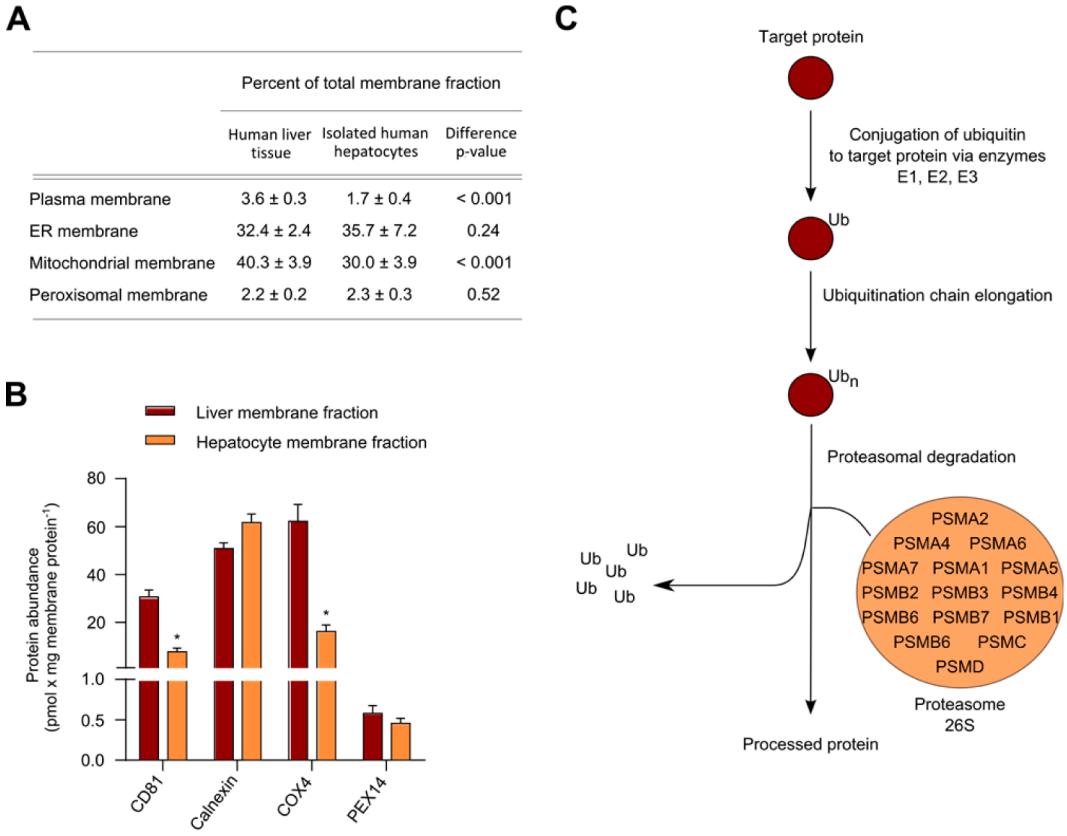


**Figure 2.** Differences in the membrane proteomes of human liver tissue and isolated hepatocytes. (A) Relative amounts of different membrane types for the two groups. (B) Protein abundance levels of commonly used membrane markers. The plasma membrane and mitochondrial membrane markers CD81 and COX4 were less abundant in hepatocytes compared to amounts in liver tissue ($p < 0.01$), while the endoplasmic reticulum (ER) and peroxisomal membrane markers calnexin and PEX14 showed comparable levels. (C) Outline of the protein ubiquitination pathway associated with differentially expressed proteins. The degradation of proteins via the pathway involves conjugation of ubiquitin moieties to the target protein followed by proteasomal degradation of the polyubiquitinated protein.

### Prediction of Transporter-Mediated Hepatic Uptake Clearance of Pitavastatin from Protein Abundance Data

The reduced transporter abundance in the plasma membrane of isolated hepatocytes could explain the frequent underpredictions of liver CL for compounds that rely on transport proteins for their hepatic uptake.[36,37] We therefore investigated to what extent the reduced abundance would affect the uptake CL of pitavastatin, a drug that is extracted from the blood circulation by four hepatic transporters. Transport activity was measured in HEK293 cells stably transfected with each of the uptake transporters. This allowed us to determine the kinetics for each transporter in isolation. The data were subsequently extrapolated to isolated hepatocytes and liver tissue by applying scaling factors for the differences in transport protein expression, as outlined in Figure 4A. The prediction parameters are summarized in Table S2 in the Supporting Information.

Active-transporter-mediated uptake CL of pitavastatin was determined to be 3-fold lower in hepatocytes than liver tissue (Figure 4B). This difference can mainly be attributed to a decreased abundance of OATP1B1, which was identified as the major uptake transporter of pitavastatin (61% and 62% of active uptake in liver and hepatocytes, respectively). In contrast to OATP1B1, the bile acid transporter NTCP was predicted to play a minor role in pitavastatin uptake (<10%).

To challenge our results, we used quantitative transporter data from an independent study of pitavastatin uptake in a pooled batch of human hepatocytes.[32,33] By scaling our kinetic data to the reported transporter abundances, we predicted a transporter-mediated CL close to the previously reported experimental value (22 versus 29 $\mu$L/min/mg protein). These results provide strong support for our scaling approach.

## DISCUSSION

The possibilities and limitations associated with the use of hepatocytes in various culture configurations depend on changes initiated already during isolation of these cells.[17] An understanding of such changes is thus crucial for a correct interpretation of in vitro data in studies of hepatic drug transport, metabolism, and toxicity. Herein, we used quantitative label-free shotgun proteomics to compare snap-frozen freshly isolated human hepatocytes with snap-frozen liver tissue for differences in their membrane proteome.

Overall there was a good global correlation in protein abundance for the two sample types, allowing the identification of stably expressed proteins (Figure 1F). Of these, STIM1, HSD17B4, TECR, SACM1L, ESYT2, VCP, and PDIA6 also displayed low variability in mRNA expression across various tissue types.[38] Hence, we propose that they can be used as internal standards when studying protein abundance in the liver and possibly other tissues as well. Proteins with high interindividual variability were found to be linked to immune response processes, which agrees with a proteome-wide analysis of cell lines derived from a larger number of individuals.[39] These types of proteins are also expected to display high intraindividual variability following infections and other stimuli.[40]


DOI: 10.1021/acs.jproteome.5b00334
J. Proteome Res. 2015, 14, 3305−3314

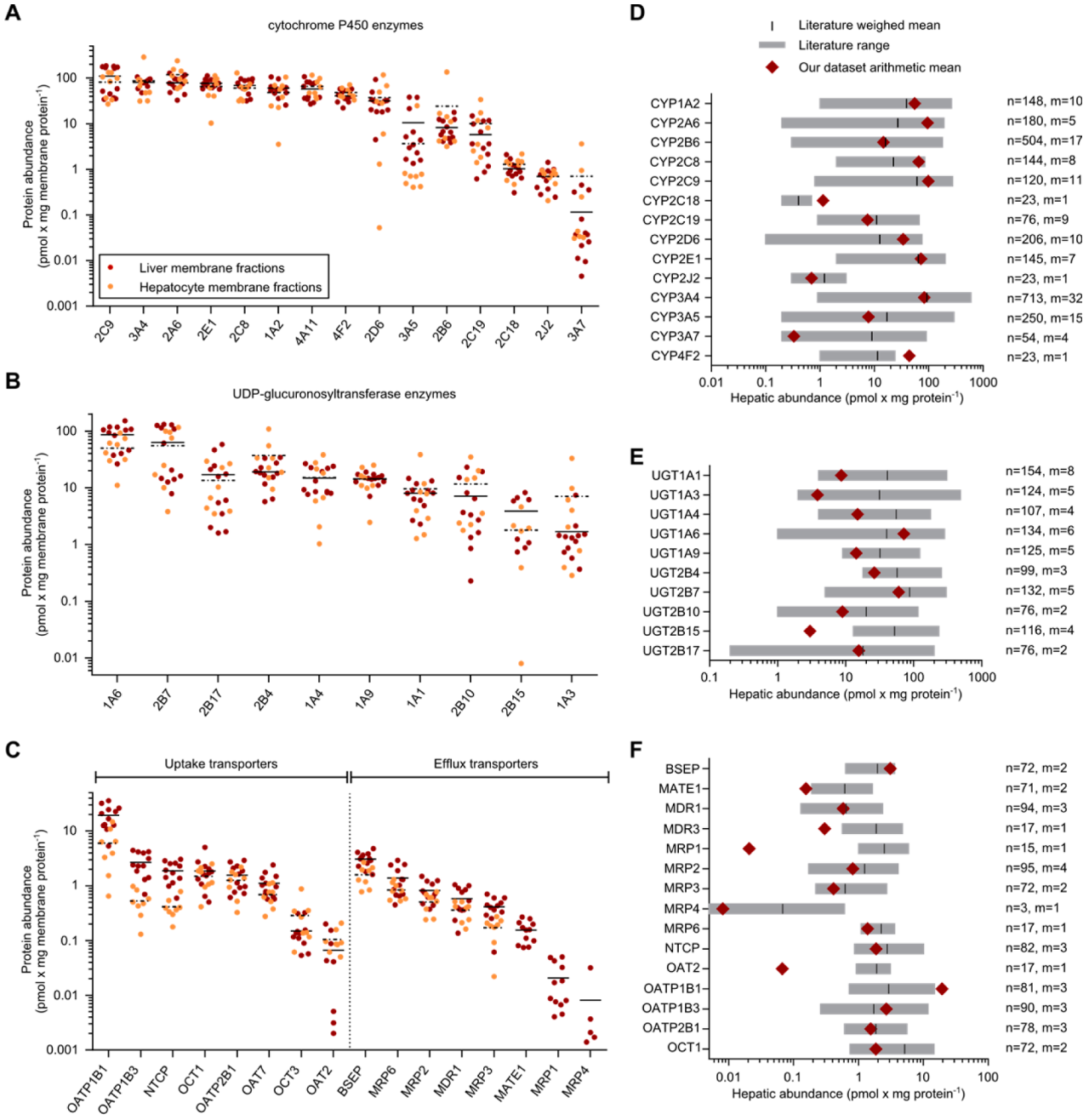


**Figure 3.** Abundances of important drug-metabolizing enzymes and transporters in human liver and hepatocytes. Interindividual expression of drug-metabolizing cytochrome P450 (CYP) enzymes (A), uridine 5′-diphospho-glucuronosyltransferase (UGT) enzymes (B), and drug transporters (C). The solid and dotted lines represent the arithmetic means for the liver and hepatocyte samples, respectively. Comparison of CYP (D) and UGT (E) enzyme abundances with the range and weighed means from two recent meta-analyses.[27,28] (F) Comparison of transporter abundances with reported values from the literature. *n*, number of liver samples; *m*, number of studies.

Ischemia and reperfusion events during hepatic surgery are known to induce oxidative stress; much of the damage from ischemic events occurs during reoxygenation as a result of increased reactive oxygen species (ROS) production.[41] The oxidative stress is further enhanced during hepatocyte isolation. For instance, hepatocytes lose as much as half of their initial total and reduced glutathione levels during isolation,[16] largely due to the scavenging of excess ROS. ROS, in turn, can directly induce the opening of mitochondrial permeability transition pores, leading to the depolarization of the inner mitochondrial membrane and the uncoupling of the oxidative phosphorylation process. In addition, the pore openings allow the release of intramitochondrial molecules, such as coenzyme A.[42] This release may promote palmitoylation of membrane-associated proteins, which is suggested to cause membrane protein clustering and invagination of the cell membrane, followed by internalization.[43,44] Plasma membrane invagination and internalization have been observed by electron microscopy during hepatocyte isolations.[45] Our data support all of these findings. Differentially expressed proteins were associated with oxidative stress responses and mitochondrial dysfunction. The lower mitochondrial protein fraction in the isolated hepatocytes than in the liver tissue is likely a result of mitochondrial membrane rupture due to rapid swelling in response to the increased permeability of the mitochondrial membranes.[46]



DOI: 10.1021/acs.jproteome.5b00334
*J. Proteome Res.* 2015, 14, 3305−3314

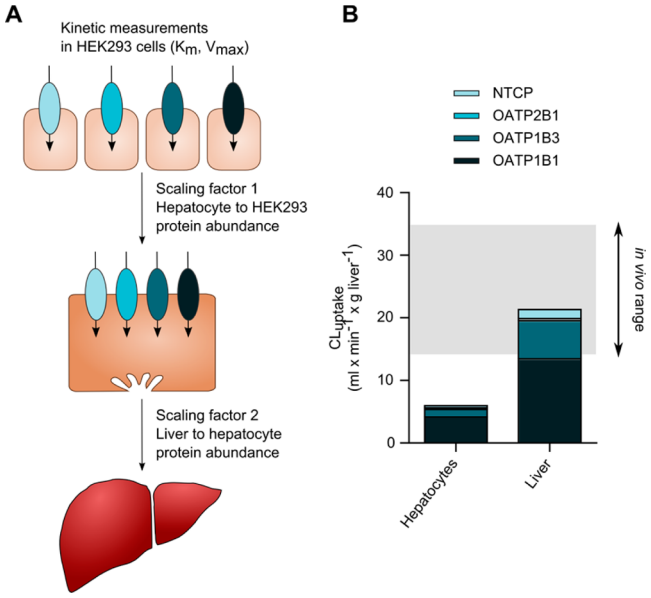


**Figure 4.** Predictions of pitavastatin uptake clearance ($CL_{uptake}$) from protein expression data. (A) Outline of the in vitro−in vivo scaling approach. (B) Transporter-mediated CL in isolated hepatocytes was predicted to be 3-fold lower than in liver tissue.

The turnover of plasma membrane proteins and proteins that enter the cell by endocytosis is generally believed to involve subsequent proteolysis within the lysosomes. However, our analysis found no association with the lysosomal pathway. Instead, our results indicated that the internalized plasma membrane proteins are degraded by the proteasomes via the protein ubiquitination pathway. Both lysosomal and proteasomal degradation are fast processes that permit a cell to adapt to new physiological conditions. Proteasomal degradation can occur within minutes.[47,48] There is at least one well-documented example in which ubiquitination targets a plasma membrane protein for proteasomal degradation−−hepatocyte growth factor receptor (HGFR).[49] In agreement with this finding, HGFR was below detectable levels in the isolated hepatocytes but at measurable levels in our liver samples. Proteasomal degradation of internalized plasma membrane proteins does not exclude the involvement of lysosomal degradation; the proteasome might aid in degrading cytosolic parts of the membrane proteins on their way to the lysosome.[50] In fact, a previous study shows that both lysosmal and proteasomal degradation occur in isolated rat hepatocytes at a rate that is much higher than protein synthesis, resulting in a net loss of protein.[51] The exact mechanisms underlying the membrane protein degradation in our study remains to be investigated.

Among the affected plasma membrane proteins, we found transport proteins important for hepatic drug elimination.[52] Importantly, the most affected transporters are exclusively expressed in hepatocytes. This indicates that the loss of plasma membrane proteins is not a result of the presence of other less abundant cell types in the liver with partially overlapping membrane proteomes. The lower abundances of transport proteins in hepatocytes as compared to liver tissue is also in agreement with other studies on the expression of smaller subsets of transporters.[33,53−55]

The reduced transporter abundance in isolated hepatocytes could explain the frequently reported underpredictions of in vivo uptake CL from hepatocyte experiments.[36,55] Current approaches to address this discrepancy rely on the use of empirical and regression-based scaling factors that fail to provide a mechanistic understanding of the in vitro−in vivo difference. In addition, these empirical scaling factors are often compound-specific and hence, suboptimal for predicting the in vivo CL of new drug entities. In our study, we reasoned that the difference in transport protein abundance for the isolated hepatocytes and liver tissue may serve as a more generic scaling factor for improved in vivo predictability. We therefore selected a drug, pitavastatin, which is predominantly dependent on transporters for its hepatic CL. As expected, the pitavastatin uptake CL in isolated hepatocytes was 2- to 6-fold lower than the reported clinical range (14−35 mL/min/g liver).[56] However, by accounting for the reduced transporter abundance, we were able to correctly predict the pitavastatin uptake CL in humans. Our in vitro−in vivo scaling approach relies on a linear correlation between transport protein expression and activity, which is supported by a recent study.[57] We tentatively conclude that more accurate in vivo predictions can be obtained by taking into account differences in protein abundance. Importantly, this scaling approach is generic and can therefore be applied to other proteins or sets of proteins determining drug exposure.

In summary, these data provide the first comparative quantitative proteomic analysis of human liver tissue and freshly isolated hepatocytes at a global level. Besides providing quantitative data for, for example, systems biology applications, our results can guide future efforts to obtain hepatic in vitro models that are more in-vivo-like. Our pathway analysis confirms previous findings regarding oxidative stress and provides novel insights into other processes that may be associated with isolating these primary cells, such as the degradation of plasma membrane proteins. Our results emphasize the need for strategies to reduce the oxidative stress, thereby potentially preserving the plasma membrane proteins and approaching the normal in vivo functions of these primary cells in culture. Meanwhile, quantifications of differences in protein expression for isolated hepatocytes and the liver counterpart can be used to scale in vitro data to the in vivo situation as exemplified by our pitavastatin CL predictions.

## ■ ASSOCIATED CONTENT

### Supporting Information

Figure S1: Cumulative protein mass. Figure S2: Outline of the NRF2-mediated oxidative stress response pathway. Table S1: Meta-analysis of transport protein abundance in human liver tissue. Table S2: Parameters for the in vitro−in vivo scaling of pitavastatin uptake clearance. The mass spectrometry data has been deposited to the ProteomeXchange Consortium[58] via the PRIDE partner repository with the data set identifier PXD002235. The Supporting Information is available free of charge on the ACS Publications website at DOI: 10.1021/acs.jproteome.5b00334.

## ■ AUTHOR INFORMATION

### Corresponding Author

*E-mail: per.artursson@farmaci.uu.se. Tel: +46184714471. Fax: +46184714223.

### Notes

The authors declare no competing financial interest.

## ■ ACKNOWLEDGMENTS

This work was supported by the Swedish Research Council (grant approval no. 2822), the Lars Hierta Memorial Foundation, O.E. and Edla Johansson's Scientific Foundation,



DOI: 10.1021/acs.jproteome.5b00334
J. Proteome Res. 2015, 14, 3305−3314

and the Max Planck Society for the Advancement of Science. The authors thank Dr. Achour for the measured ranges in CYP and UGT abundance from the published studies included in his meta-analyses, Dr. Sato for the measured range of UGT enzymes in his study, Dr. Wang for the measured range of transporters in his publication, and Prof. Matthias Mann for continuous support.

## ■ ABBREVIATIONS

ADME, absorption, distribution, metabolism, and excretion; LC−MS/MS, liquid chromatography-tandem mass spectrometry; CYP, cytochrome P450; UGT, uridine 5′-diphospho-glucuronosyltransferase; HEK293, human embryonic kidney 293; $V_{max}$, maximal transport rate; CL, clearance; GO, gene ontology; OATP, organic anion-transporting polypeptide; NTCP, sodium−taurocholate cotransporting polypeptide; ROS, reactive oxygen species

## ■ REFERENCES

(1) *Drug-Induced Liver Injury: Premarketing Clinical Evaluation*; *Guidance for Industry*; U.S. Food and Drug Administration: Rockville, MD, 2009.
(2) Watkins, P. B. Drug safety sciences and the bottleneck in drug development. *Clin. Pharmacol. Ther.* **2011**, *89* (6), 788−790.
(3) Berger, D. R.; Ware, B. R.; Davidson, M. D.; Allsup, S. R.; Khetani, S. R. Enhancing the functional maturity of induced pluripotent stem cell-derived human hepatocytes by controlled presentation of cell-cell interactions in vitro. *Hepatology* **2015**, *61* (4), 1370−1381.
(4) Chen, Y. F.; Tseng, C. Y.; Wang, H. W.; Kuo, H. C.; Yang, V. W.; Lee, O. K. Rapid generation of mature hepatocyte-like cells from human induced pluripotent stem cells by an efficient three-step protocol. *Hepatology* **2012**, *55* (4), 1193−1203.
(5) Baxter, M.; Withey, S.; Harrison, S.; Segeritz, C. P.; Zhang, F.; Atkinson-Dell, R.; Rowe, C.; Gerrard, D. T.; Sison-Young, R.; Jenkins, R.; Henry, J.; Berry, A. A.; Mohamet, L.; Best, M.; Fenwick, S. W.; Malik, H.; Kitteringham, N. R.; Goldring, C. E.; Piper Hanley, K.; Vallier, L.; Hanley, N. A. Phenotypic and functional analyses show stem cell-derived hepatocyte-like cells better mimic fetal rather than adult hepatocytes. *J. Hepatol.* **2015**, *62* (3), 581−589.
(6) Sim, S. C.; Ingelman-Sundberg, M. Pharmacogenomic biomarkers: new tools in current and future drug therapy. *Trends Pharmacol. Sci.* **2011**, *32* (2), 72−81.
(7) Beck, M.; Claassen, M.; Aebersold, R. Comprehensive proteomics. *Curr. Opin. Biotechnol.* **2011**, *22* (1), 3−8.
(8) Wisniewski, J. R.; Ostasiewicz, P.; Dus, K.; Zielinska, D. F.; Gnad, F.; Mann, M. Extensive quantitative remodeling of the proteome between normal colon tissue and adenocarcinoma. *Mol. Syst. Biol.* **2012**, *8*, 611.
(9) Wisniewski, J. R.; Hein, M. Y.; Cox, J.; Mann, M. A 'proteomic ruler' for protein copy number and concentration estimation without spike-in standards. *Mol. Cell. Proteomics* **2014**, *13* (12), 3497−3506.
(10) Boess, F.; Kamber, M.; Romer, S.; Gasser, R.; Muller, D.; Albertini, S.; Suter, L. Gene expression in two hepatic cell lines, cultured primary hepatocytes, and liver slices compared to the in vivo liver gene expression in rats: possible implications for toxicogenomics use of in vitro systems. *Toxicol. Sci.* **2003**, *73* (2), 386−402.
(11) Richert, L.; Liguori, M. J.; Abadie, C.; Heyd, B.; Mantion, G.; Halkic, N.; Waring, J. F. Gene expression in human hepatocytes in suspension after isolation is similar to the liver of origin, is not affected by hepatocyte cold storage and cryopreservation, but is strongly changed after hepatocyte plating. *Drug Metab. Dispos.* **2006**, *34* (5), 870−879.
(12) Vogel, C.; Marcotte, E. M. Insights into the regulation of protein abundance from proteomic and transcriptomic analyses. *Nat. Rev. Genet.* **2012**, *13* (4), 227−232.
(13) Wimmer, H.; Gundacker, N. C.; Griss, J.; Haudek, V. J.; Stattner, S.; Mohr, T.; Zwickl, H.; Paulitschke, V.; Baron, D. M.; Trittner, W.; Kubicek, M.; Bayer, E.; Slany, A.; Gerner, C. Introducing the CPL/MUW proteome database: interpretation of human liver and liver cancer proteome profiles by referring to isolated primary cells. *Electrophoresis* **2009**, *30* (12), 2076−2089.
(14) Rowe, C.; Goldring, C. E.; Kitteringham, N. R.; Jenkins, R. E.; Lane, B. S.; Sanderson, C.; Elliott, V.; Platt, V.; Metcalfe, P.; Park, B. K. Network analysis of primary hepatocyte dedifferentiation using a shotgun proteomics approach. *J. Proteome Res.* **2010**, *9* (5), 2658−2668.
(15) Rowe, C.; Gerrard, D. T.; Jenkins, R.; Berry, A.; Durkin, K.; Sundstrom, L.; Goldring, C. E.; Park, B. K.; Kitteringham, N. R.; Hanley, K. P.; Hanley, N. A. Proteome-wide analyses of human hepatocytes during differentiation and dedifferentiation. *Hepatology* **2013**, *58* (2), 799−809.
(16) Musallam, L.; Ethier, C.; Haddad, P. S.; Denizeau, F.; Bilodeau, M. Resistance to Fas-induced apoptosis in hepatocytes: role of GSH depletion by cell isolation and culture. *Am. J. Physiol Gastrointest Liver Physiol* **2002**, *283* (3), G709−718.
(17) Elaut, G.; Henkens, T.; Papeleu, P.; Snykers, S.; Vinken, M.; Vanhaecke, T.; Rogiers, V. Molecular mechanisms underlying the dedifferentiation process of isolated hepatocytes and their cultures. *Curr. Drug Metab* **2006**, *7* (6), 629−660.
(18) LeCluyse, E. L.; Alexandre, E. Isolation and culture of primary hepatocytes from resected human liver tissue. *Methods Mol. Biol.* **2010**, *640*, 57−82.
(19) Wisniewski, J. R. Protocol to enrich and analyze plasma membrane proteins from frozen tissues. *Methods Mol. Biol.* **2008**, *432*, 175−183.
(20) Wisniewski, J. R.; Zielinska, D. F.; Mann, M. Comparison of ultrafiltration units for proteomic and N-glycoproteomic analysis by the filter-aided sample preparation method. *Anal. Biochem.* **2011**, *410* (2), 307−309.
(21) Wisniewski, J. R.; Zougman, A.; Nagaraj, N.; Mann, M. Universal sample preparation method for proteome analysis. *Nat. Methods* **2009**, *6* (5), 359−362.
(22) Wisniewski, J. R.; Zougman, A.; Mann, M. Combination of FASP and StageTip-based fractionation allows in-depth analysis of the hippocampal membrane proteome. *J. Proteome Res.* **2009**, *8* (12), 5674−5678.
(23) Rappsilber, J.; Ishihama, Y.; Mann, M. Stop and go extraction tips for matrix-assisted laser desorption/ionization, nanoelectrospray, and LC/MS sample pretreatment in proteomics. *Anal. Chem.* **2003**, *75* (3), 663−670.
(24) Wisniewski, J. R.; Gaugaz, F. Z. Fast and sensitive total protein and Peptide assays for proteomic analysis. *Anal. Chem.* **2015**, *87* (8), 4110−4116.
(25) Cox, J.; Mann, M. MaxQuant enables high peptide identification rates, individualized p.p.b.-range mass accuracies and proteome-wide protein quantification. *Nat. Biotechnol.* **2008**, *26* (12), 1367−1372.
(26) Wisniewski, J. R.; Rakus, D. Multi-enzyme digestion FASP and the 'Total Protein Approach'-based absolute quantification of the Escherichia coli proteome. *J. Proteomics* **2014**, *109C*, 322−331.
(27) Achour, B.; Barber, J.; Rostami-Hodjegan, A. Expression of hepatic drug-metabolizing cytochrome p450 enzymes and their intercorrelations: a meta-analysis. *Drug Metab. Dispos.* **2014**, *42* (8), 1349−1356.
(28) Achour, B.; Rostami-Hodjegan, A.; Barber, J. Protein expression of various hepatic uridine 5′-diphosphate glucuronosyltransferase (UGT) enzymes and their inter-correlations: a meta-analysis. *Biopharm. Drug Dispos.* **2014**, *35* (6), 353−361.
(29) Sato, Y.; Nagata, M.; Tetsuka, K.; Tamura, K.; Miyashita, A.; Kawamura, A.; Usui, T. Optimized methods for targeted peptide-based quantification of human uridine 5′-diphosphate-glucuronosyltransferases in biological specimens using liquid chromatography-tandem mass spectrometry. *Drug Metab. Dispos.* **2014**, *42* (5), 885−889.
(30) Vildhede, A.; Karlgren, M.; Svedberg, E. K.; Wisniewski, J. R.; Lai, Y.; Noren, A.; Artursson, P. Hepatic uptake of atorvastatin: influence of variability in transporter expression on uptake clearance and drug-drug interactions. *Drug Metab. Dispos.* **2014**, *42* (7), 1210−1218.
(31) Karlgren, M.; Vildhede, A.; Norinder, U.; Wisniewski, J. R.; Kimoto, E.; Lai, Y.; Haglund, U.; Artursson, P. Classification of inhibitors of hepatic organic anion transporting polypeptides (OATPs): influence of


DOI: 10.1021/acs.jproteome.5b00334
*J. Proteome Res.* 2015, 14, 3305−3314

protein expression on drug-drug interactions. *J. Med. Chem.* **2012**, *55* (10), 4740−4763.
(32) Bi, Y. A.; Qiu, X.; Rotter, C. J.; Kimoto, E.; Piotrowski, M.; Varma, M. V.; Ei-Kattan, A. F.; Lai, Y. Quantitative assessment of the contribution of sodium-dependent taurocholate co-transporting polypeptide (NTCP) to the hepatic uptake of rosuvastatin, pitavastatin and fluvastatin. *Biopharm. Drug Dispos.* **2013**, *34* (8), 452−461.
(33) Kimoto, E.; Yoshida, K.; Balogh, L. M.; Bi, Y. A.; Maeda, K.; El-Kattan, A.; Sugiyama, Y.; Lai, Y. Characterization of Organic Anion Transporting Polypeptide (OATP) Expression and Its Functional Contribution to the Uptake of Substrates in Human Hepatocytes. *Mol. Pharmaceutics* **2012**, *9* (12), 3535−3542.
(34) Urdzik, J. Colorectal Cancer Liver Metastases: Effects of Chemotherapy on Liver Parenchyma and Resections. Doctoral Thesis (Comprehensive Summary), Uppsala University, Uppsala, Sweden, 2014.
(35) Schroder, A.; Klein, K.; Winter, S.; Schwab, M.; Bonin, M.; Zell, A.; Zanger, U. M. Genomics of ADME gene expression: mapping expression quantitative trait loci relevant for absorption, distribution, metabolism and excretion of drugs in human liver. *Pharmacogenomics J.* **2013**, *13* (1), 12−20.
(36) Menochet, K.; Kenworthy, K. E.; Houston, J. B.; Galetin, A. Use of mechanistic modeling to assess interindividual variability and interspecies differences in active uptake in human and rat hepatocytes. *Drug Metab. Dispos.* **2012**, *40* (9), 1744−1756.
(37) Poirier, A.; Funk, C.; Scherrmann, J. M.; Lave, T. Mechanistic modeling of hepatic transport from cells to whole body: application to napsagatran and fexofenadine. *Mol. Pharmaceutics* **2009**, *6* (6), 1716−1733.
(38) Eisenberg, E.; Levanon, E. Y. Human housekeeping genes, revisited. *Trends Genet.* **2013**, *29* (10), 569−574.
(39) Wu, L.; Candille, S. I.; Choi, Y.; Xie, D.; Jiang, L.; Li-Pook-Than, J.; Tang, H.; Snyder, M. Variation and genetic control of protein abundance in humans. *Nature* **2013**, *499* (7456), 79−82.
(40) Chen, R.; Mias, G. I.; Li-Pook-Than, J.; Jiang, L.; Lam, H. Y.; Miriami, E.; Karczewski, K. J.; Hariharan, M.; Dewey, F. E.; Cheng, Y.; Clark, M. J.; Im, H.; Habegger, L.; Balasubramanian, S.; O'Huallachain, M.; Dudley, J. T.; Hillenmeyer, S.; Haraksingh, R.; Sharon, D.; Euskirchen, G.; Lacroute, P.; Bettinger, K.; Boyle, A. P.; Kasowski, M.; Grubert, F.; Seki, S.; Garcia, M.; Whirl-Carrillo, M.; Gallardo, M.; Blasco, M. A.; Greenberg, P. L.; Snyder, P.; Klein, T. E.; Altman, R. B.; Butte, A. J.; Ashley, E. A.; Gerstein, M.; Nadeau, K. C.; Tang, H.; Snyder, M. Personal omics profiling reveals dynamic molecular and medical phenotypes. *Cell* **2012**, *148* (6), 1293−1307.
(41) Garcea, G.; Gescher, A.; Steward, W.; Dennison, A.; Berry, D. Oxidative stress in humans following the Pringle manoeuvre. *Hepatobiliary Pancreat Dis Int.* **2006**, *5* (2), 210−214.
(42) Halestrap, A. P.; Clarke, S. J.; Javadov, S. A. Mitochondrial permeability transition pore opening during myocardial reperfusion–a target for cardioprotection. *Cardiovasc. Res.* **2004**, *61* (3), 372−385.
(43) Lin, M. J.; Fine, M.; Lu, J. Y.; Hofmann, S. L.; Frazier, G.; Hilgemann, D. W. Massive palmitoylation-dependent endocytosis during reoxygenation of anoxic cardiac muscle. *eLife* **2013**, *2*, e01295.
(44) Hilgemann, D. W.; Fine, M.; Linder, M. E.; Jennings, B. C.; Lin, M. J. Massive endocytosis triggered by surface membrane palmitoylation under mitochondrial control in BHK fibroblasts. *eLife* **2013**, *2*, e01293.
(45) Berry, M. N.; Friend, D. S. High-yield preparation of isolated rat liver parenchymal cells: a biochemical and fine structural study. *J. Cell Biol.* **1969**, *43* (3), 506−520.
(46) Kim, J. S.; Qian, T.; Lemasters, J. J. Mitochondrial permeability transition in the switch from necrotic to apoptotic cell death in ischemic rat hepatocytes. *Gastroenterology* **2003**, *124* (2), 494−503.
(47) Verma, R.; McDonald, H.; Yates, J. R., 3rd; Deshaies, R. J. Selective degradation of ubiquitinated Sic1 by purified 26S proteasome yields active S phase cyclin-Cdk. *Mol. Cell* **2001**, *8* (2), 439−448.
(48) Peth, A.; Nathan, J. A.; Goldberg, A. L. The ATP costs and time required to degrade ubiquitinated proteins by the 26 S proteasome. *J. Biol. Chem.* **2013**, *288* (40), 29215−29222.
(49) Jeffers, M.; Taylor, G. A.; Weidner, K. M.; Omura, S.; Vande Woude, G. F. Degradation of the Met tyrosine kinase receptor by the ubiquitin-proteasome pathway. *Mol. Cell. Biol.* **1997**, *17* (2), 799−808.
(50) Strous, G. J.; Govers, R. The ubiquitin-proteasome system and endocytosis. *J. Cell Sci.* **1999**, *112* (Pt 10), 1417−1423.
(51) Seglen, P. O.; Grinde, B.; Solheim, A. E. Inhibition of the lysosomal pathway of protein degradation in isolated rat hepatocytes by ammonia, methylamine, chloroquine and leupeptin. *Eur. J. Biochem.* **1979**, *95* (2), 215−225.
(52) Giacomini, K. M.; Huang, S. M.; Tweedie, D. J.; Benet, L. Z.; Brouwer, K. L.; Chu, X.; Dahlin, A.; Evers, R.; Fischer, V.; Hillgren, K. M.; Hoffmaster, K. A.; Ishikawa, T.; Keppler, D.; Kim, R. B.; Lee, C. A.; Niemi, M.; Polli, J. W.; Sugiyama, Y.; Swaan, P. W.; Ware, J. A.; Wright, S. H.; Yee, S. W.; Zamek-Gliszczynski, M. J.; Zhang, L. Membrane transporters in drug development. *Nat. Rev. Drug Discovery* **2010**, *9* (3), 215−236.
(53) Bow, D. A.; Perry, J. L.; Miller, D. S.; Pritchard, J. B.; Brouwer, K. L. Localization of P-gp (Abcb1) and Mrp2 (Abcc2) in freshly isolated rat hepatocytes. *Drug Metab. Dispos.* **2007**, *36* (1), 198−202.
(54) Roelofsen, H.; Bakker, C. T.; Schoemaker, B.; Heijn, M.; Jansen, P. L.; Oude Elferink, R. P. J. Redistribution of canalicular organic anion transport activity in isolated and cultured rat hepatocytes. *Hepatology* **1995**, *21* (6), 1649−1657.
(55) Lundquist, P.; Loof, J.; Sohlenius-Sternbeck, A. K.; Floby, E.; Johansson, J.; Bylund, J.; Hoogstraate, J.; Afzelius, L.; Andersson, T. B. The impact of solute carrier (SLC) drug uptake transporter loss in human and rat cryopreserved hepatocytes on clearance predictions. *Drug Metab. Dispos.* **2014**, *42* (3), 469−480.
(56) Watanabe, T.; Kusuhara, H.; Maeda, K.; Kanamaru, H.; Saito, Y.; Hu, Z.; Sugiyama, Y. Investigation of the rate-determining process in the hepatic elimination of HMG-CoA reductase inhibitors in rats and humans. *Drug Metab. Dispos.* **2010**, *38* (2), 215−222.
(57) Kumar, V.; Prasad, B.; Patilea, G.; Gupta, A.; Salphati, L.; Evers, R.; Hop, C. E.; Unadkat, J. D. Quantitative Transporter Proteomics by LC-MS/MS: Addressing Methodological Issues of Plasma Membrane Isolation and Expression-activity Relationship. *Drug Metab. Dispos.* **2014**, *43* (2), 284−288.
(58) Vizcaino, J. A.; Deutsch, E. W.; Wang, R.; Csordas, A.; Reisinger, F.; Rios, D.; Dianes, J. A.; Sun, Z.; Farrah, T.; Bandeira, N.; Binz, P. A.; Xenarios, I.; Eisenacher, M.; Mayer, G.; Gatto, L.; Campos, A.; Chalkley, R. J.; Kraus, H. J.; Albar, J. P.; Martinez-Bartolome, S.; Apweiler, R.; Omenn, G. S.; Martens, L.; Jones, A. R.; Hermjakob, H. ProteomeXchange provides globally coordinated proteomics data submission and dissemination. *Nat. Biotechnol.* **2014**, *32* (3), 223−226.


DOI: 10.1021/acs.jproteome.5b00334
*J. Proteome Res.* 2015, 14, 3305−3314